Anal. Chem. **2010,** *82,* 5125–5133

Quantum Dot-Based Immunochromatographic Fluorescent Biosensor for Biomonitoring Trichloropyridinol, a Biomarker of Exposure to Chlorpyrifos

Zhexiang Zou,[†,‡] Dan Du,[‡,⊥] Jun Wang,[*,‡] Jordan N. Smith,[‡] Charles Timchalk,[‡] Yaoqun Li,[*,†] and Yuehe Lin[*,‡]

Department of Chemistry and Key Laboratory of Analytical Sciences, College of Chemistry and Chemical Engineering, Xiamen University, Xiamen 361005 China, and Pacific Northwest National Laboratory, Richland, Washington 99352, and College of Chemistry, Central China Normal University, Wuhan 430039 China

A novel and portable fluorescent sensor that integrates an immunochromatographic test strip assay (ITSA) with a quantum dot (QD) label and a test strip reader was described in this study for simple, rapid, and sensitive biomonitoring of an organophosphorus pesticide metabolite. The principle of this sensor is based on a competitive immunoreaction that was performed on an immunochromatographic test strip, where analytes compete with competitors (QD-conjugated analogs) to bind to antibodies on a test zone. Captured QDs serve as signal vehicles for fluorescent readout. In this work, 3,5,6-trichloropyridinol (TCP) is used as a model analyte to demonstrate the performance of the immunosensor. QD−TCP conjugates were synthesized and characterized with X-ray photoelectron spectroscopy (XPS) and fluorescence spectroscopy. Some parameters (e.g., the amount of QD-modified TCP and immunoreaction time) that govern sensitivity and reproducibility of ITSA were optimized. Under optimal conditions, the sensor has a wide dynamic range and is capable of detecting a minimum 1.0 ng/mL TCP standard analyte in 15 min. The sensor has been successfully applied for detection of TCP spiked in rat plasma with average recovery of 102.0%. Results demonstrate that this sensor provides a rapid, clinically accurate, and quantitative tool for TCP detection and shows great promise for in-field and point-of-care (POC) quantitative testing and screening for metabolite biomarkers, e.g., TCP, for humans exposed to pesticides.

Recent years have witnessed considerable efforts to develop point-of-care (POC) or field-deployable biosensors because of their widespread potential applications in clinical diagnosis,[1,2] environmental monitoring,[3,4] food analysis,[5,6] forensic diagnosis,[7] and national security screening.[8,9] In comparison to laboratory-oriented large analytical instruments, the biggest advantage of biosensors is that they are portable and rapidly responsive; therefore, they can be used on site including at a patient's bedside, physician's office, and home providing real-time results and avoiding costly sample transportation and lengthy waiting time for results. Since biosensors are sensitive and selective, they only need a small sample volume, which is directly analyzed, thus, avoiding tedious sample preparation associated with more standard analytical methods. Additionally, biosensors generally are simple, user-friendly, and inexpensive and do not need well-trained personnel, which are mostly associated with those large analytical instruments in lab.

Currently, most biosensors are based on optical[10−12] or electrochemical[13−15] readout systems. Some of these are commercially available such as glucose meters[16,17] and cholesterol meters,[18] among others. Despite their success, there are still pressing needs for novel portable biosensors, especially for quantitation of trace amount of analytes in biological samples. A major challenge ahead for such biosensors is to

* To whom correspondence should be addressed. E-mail: jun.wang@pnl.gov (J. Wang); yqlig@xmu.edu.cn (Y. Li); yuehe.lin@pnl.gov (Y. Lin).
† Xiamen University.
‡ Pacific Northwest National Laboratory.
⊥ Central China Normal University.

(1) Lin, J. H.; Ju, H. X. *Biosens. Bioelectron.* **2005**, *20*, 1461–1470.
(2) Wang, Y.; Xu, H.; Zhang, J. M.; Li, G. *Sensors* **2008**, *8*, 2043–2081.
(3) Reardon, K. F.; Zhong, Z.; Lear, K. L. *Adv. Biochem. Eng. Biotechnol.* **2009**, *116*, 99−123.
(4) Rocha-Gaso, M. I.; March-Iborra, C.; Montoya-Baides, A.; Arnau-Vives, A. *Sensors* **2009**, *9*, 5740–5769.
(5) Arshak, K.; Velusamy, V.; Korostynska, O.; Oliwa-Stasiak, K.; Adley, C. *IEEE Sens. J.* **2009**, *9*, 1942–1951.
(6) Viswanathan, S.; Radecka, H.; Radecki, J. *Monatsh. Chem.* **2009**, *140*, 891–899.
(7) Frasconi, M.; Mazzarino, M.; Botre, F.; Mazzei, F. *Anal. Bioanal. Chem.* **2009**, *394*, 2151–2159.
(8) Wang, H.; Wang, J.; Timchalk, C.; Lin, Y. H. *Anal. Chem.* **2008**, *80*, 8477–8484.
(9) Wang, J.; Timchalk, C.; Lin, Y. H. *Environ. Sci. Technol.* **2008**, *42*, 2688–2693.
(10) Fan, X. D.; White, I. M.; Shopoua, S. I.; Zhu, H. Y.; Suter, J. D.; Sun, Y. Z. *Anal. Chim. Acta* **2008**, *620*, 8–26.
(11) Fraser, D. *Med. Device Technol.* **1995**, *6*, 28–32, 34.
(12) Wang, H. X.; Nakata, E.; Hamachi, I. *ChemBioChem* **2009**, *10*, 2560–2577.
(13) Privett, B. J.; Shin, J. H.; Schoenfisch, M. H. *Anal. Chem.* **2008**, *80*, 4499–4517.
(14) Wang, J. *Anal. Chim. Acta* **2002**, *469*, 63–71.
(15) Guth, U.; Vonau, W.; Zosel, J. *Meas. Sci. Technol.* **2009**, *20*, 14.
(16) Chan, P. C. R.; Rozmanc, M.; Selden-Long, I.; Kwan, J. *Clin. Biochem.* **2009**, *42*, 1104–1112.
(17) Wang, J. *Electroanalysis* **2001**, *13*, 983–988.
(18) Test Medical Symptoms@Home, Inc.; http://www.testsymptomsathome.com/.

10.1021/ac100260m
Published on Web 05/27/2010

identify signatures from low-concentration analytes in the presence of highly abundant nonspecific biological matrixes. Additional challenges stem from the fact that some of the biosensors may suffer from biofouling on transducers that seriously hamper potential applications.[19] To address these challenges, an immunochromatographic test strip assay (ITSA) has been developed that has shown promise for quantifying low analyte concentrations in biological samples.[20−22] The significant advantage of the ITSA is that it can automatically separate analytes of interest from nonspecific biological matrixes, therefore, minimizing biological matrixes effects. Additionally, it is a one-step, straightforward assay making it simple, rapid, inexpensive, user-friendly, and adaptable to various environments. As a result, ITSA has found broad applications such as environmental monitoring,[23,24] food analysis,[25−27] and disease diagnostics.[28−31]

Importantly, the sensitivity of the ITSA could be greatly improved with signal enhancement using nanomaterials. In the early development of ITSA, colorimetric or eye detection was usually employed, wherein gold nanoparticle and some organic dyes were often used as signal reporters.[32−37] These ITSA assays generally were either qualitative or semiquantitative and were often employed for analyzing analytes of relatively high concentration in samples. However, biologically significant analytes (e.g., metabolites and protein biomarkers, among others) are often present in very low concentrations in biological fluids, and more sensitive quantitation of these analytes is highly desirable. As a result, more quantitative ITSA assays have been recently developed.[36,38−41] For example, electrochemically quantitative ITSAs have been developed using electroactive-species loaded liposome,[42] metal ion chelates,[43] inorganic nanoparticles,[44,45] and others as reporters. Quantitative fluorescent ITSA has also been developed based on fluorescent dye labels.[46−49] More recently, magnetic beads have been reported as quantitative signaling tags for developing magnetic ITSA.[50] Fluorescent ITSA, in tandem with a portable fluorescent reader, should be one of the most sensitive and promising approaches for quantifying low concentration analytes in biological samples. However, the current organic dye-based fluorescent ITSA may suffer from low emission intensity, interference, and photobleaching in the test strip membrane, which seriously compromises the sensitivity and stability of the assay and limits its application.

Quantum dots (QDs) are inorganic nanocrystals emerging as a new class of fluorescent labels for bioassays, biosensing, and bioimaging.[51−56] In comparison to organic dyes and fluorescent proteins, QDs have unique optical and electronic properties such as size-tunable light emission, superior signal brightness, resistance to photobleaching, and simultaneous excitation of multiple fluorescence colors. These properties make QDs promising for improving sensitivity and multiplexing capabilities of bioassays and biosensors.[57] In addition, quantum dot-based fluorescence technologies offer the possibility for detection in a single-molecule level because of their high sensitivity, which in turn provides an opportunity for miniaturization and high throughput screening.[58] Therefore, combining the advantage of the ITSA and the superior signal brightness and stability (e.g., resistance to photobleaching) of quantum dots will result in great improvement in sensitivity and reproducibility for these assays. As a result, the use of QD

(19) Wisniewski, N.; Reichert, M. *Colloids Surf., B: Biointerfaces* **2000**, *18*, 197–219.
(20) Sturenburg, E.; Junker, R. *Dtsch. Arzteblatt Int.* **2009**, *106*, 48–AR41.
(21) Posthuma-Trumpie, G. A.; Korf, J.; van Amerongen, A. *Anal. Bioanal. Chem.* **2009**, *393*, 569–582.
(22) Yan, Z. Q.; Zhou, L.; Zhao, Y. K.; Wang, J.; Huang, L. H.; Hu, K. X.; Liu, H. H.; Wang, H.; Guo, Z. B.; Song, Y. J.; Huang, H. J.; Yang, R. F. *Sens. Actuators, B: Chem.* **2006**, *119*, 656–663.
(23) Shim, W. B.; Yang, Z. Y.; Kim, J. Y.; Choi, J. G.; Je, J. H.; Kang, S. J.; Kolosova, A. Y.; Eremin, S. A.; Chung, D. H. *J. Agric. Food Chem.* **2006**, *54*, 9728–9734.
(24) Bogdanovic, J.; Koets, M.; Sander, I.; Wouters, I.; Meijster, T.; Heederik, D.; van Amerongen, A.; Doekes, G. *J. Allergy Clin. Immunol.* **2006**, *118*, 1157–1163.
(25) Watanabe, H.; Satake, A.; Kido, Y.; Tsuji, A. *Anal. Chim. Acta* **2001**, *437*, 31–38.
(26) Wang, X. L.; Li, K.; Shi, D. S.; Xiong, N.; Jin, X.; Yi, J. D.; Bi, D. R. *J. Agric. Food Chem.* **2007**, *55*, 2072–2078.
(27) Wang, S.; Quan, Y.; Lee, N.; Kennedy, I. R. *J. Agric. Food Chem.* **2006**, *54*, 2491–2495.
(28) Ho, J. A. A.; Hsu, H. W. *Anal. Chem.* **2003**, *75*, 4330–4334.
(29) Huang, S. H. *Clin. Chim. Acta* **2006**, *373*, 139–143.
(30) Fernandez-Sanchez, C.; McNeil, C. J.; Rawson, K.; Nilsson, O. *Anal. Chem.* **2004**, *76*, 5649–5656.
(31) Smits, H. L.; Abdoel, T. H.; Solera, J.; Clavijo, E.; Diaz, R. *Clin. Diagn. Lab. Immunol.* **2003**, *10*, 1141–1146.
(32) Tanaka, R.; Yuhi, T.; Nagatani, N.; Endo, T.; Kerman, K.; Takamura, Y.; Tamiya, E. *Anal. Bioanal. Chem.* **2006**, *385*, 1414–1420.
(33) Klewitz, T.; Gessler, F.; Beer, H.; Pflanz, K.; Scheper, T. *Sens. Actuators, B: Chem.* **2006**, *113*, 582–589.
(34) Zhou, P.; Lu, Y. T.; Zhu, J.; Hong, J. B.; Li, B.; Zhou, J.; Gong, D.; Montoya, A. *J. Agric. Food Chem.* **2004**, *52*, 4355–4359.
(35) Shim, W. B.; Kim, K. Y.; Chung, D. H. *J. Agric. Food Chem.* **2009**, *57*, 4035–4041.
(36) Ahn-Yoon, S.; DeCory, T. R.; Baeumner, A. J.; Durst, R. A. *Anal. Chem.* **2003**, *75*, 2256–2261.
(37) Fung, K. K.; Chan, C. P. Y.; Renneberg, R. *Anal. Bioanal. Chem.* **2009**, *393*, 1281–1287.
(38) Ono, T.; Kawamura, M.; Arao, S.; Nariuchi, H. *J. Immunol. Methods* **2003**, *272*, 211–218.
(39) Esch, M. B.; Baeumner, A. J.; Durst, R. A. *Anal. Chem.* **2001**, *73*, 3162–3167.
(40) Mao, X.; Baloda, M.; Gurung, A. S.; Lin, Y. H.; Liu, G. D. *Electrochem. Commun.* **2008**, *10*, 1636–1640.
(41) Xu, H.; Mao, X.; Zeng, Q. X.; Wang, S. F.; Kawde, A. N.; Liu, G. D. *Anal. Chem.* **2009**, *81*, 669–675.
(42) Lee, K. S.; Kim, T. H.; Shin, M. C.; Lee, W. Y.; Park, J. K. *Anal. Chim. Acta* **1999**, *380*, 17–26.
(43) Lu, F.; Wang, K. H.; Lin, Y. H. *Analyst* **2005**, *130*, 1513–1517.
(44) Lin, Y. Y.; Wang, J.; Liu, G. D.; Wu, H.; Wai, C. M.; Lin, Y. H. *Biosens. Bioelectron.* **2008**, *23*, 1659–1665.
(45) Liu, G.; Lin, Y. Y.; Wang, J.; Wu, H.; Wai, C. M.; Lin, Y. *Anal. Chem.* **2007**, *79*, 7644–7653.
(46) Choi, S.; Choi, E. Y.; Kim, H. S.; Oh, S. W. *Clin. Chem.* **2004**, *50*, 1052–1055.
(47) Kim, Y. M.; Oh, S. W.; Jeong, S. Y.; Pyo, D. J.; Choi, E. Y. *Environ. Sci. Technol.* **2003**, *37*, 1899–1904.
(48) Khreich, N.; Lamourette, P.; Boutal, H.; Devilliers, K.; Creminon, C.; Volland, H. *Anal. Biochem.* **2008**, *377*, 182–188.
(49) Oh, S. W.; Kim, Y. M.; Kim, H. J.; Kim, S. J.; Cho, J. S.; Choi, E. Y. *Clin. Chim. Acta* **2009**, *406*, 18–22.
(50) Tang, D.; Sauceda, J. C.; Lin, Z.; Ott, S.; Basova, E.; Goryacheva, I.; Biselli, S.; Lin, J.; Niessner, R.; Knopp, D. *Biosens. Bioelectron.* **2009**, *25*, 514–518.
(51) Chan, W. C. W.; Nie, S. M. *Science* **1998**, *281*, 2016–2018.
(52) Chen, X. C.; Deng, Y. L.; Lin, Y.; Pang, D. W.; Qing, H.; Qu, F.; Xie, H. Y. *Nanotechnology* **2008**, *19*, 6.
(53) Smith, A. M.; Gao, X. H.; Nie, S. M. *Photochem. Photobiol.* **2004**, *80*, 377–385.
(54) Wang, J.; Liu, G. D.; Wu, H.; Lin, Y. H. *Small* **2008**, *4*, 82–86.
(55) Li, F.; Zhang, Z. P.; Peng, J.; Cui, Z. Q.; Pang, D. W.; Li, K.; Wei, H. P.; Zhou, Y. F.; Wen, J. K.; Zhang, X. E. *Small* **2009**, *5*, 718–726.
(56) Xie, M.; Liu, H. H.; Chen, P.; Zhang, Z. L.; Wang, X. H.; Xie, Z. X.; Du, Y. M.; Pan, B. Q.; Pang, D. W. *Chem. Commun.* **2005**, 5518–5520.
(57) Chan, W. C. W.; Maxwell, D. J.; Gao, X. H.; Bailey, R. E.; Han, M. Y.; Nie, S. M. *Curr. Opin. Biotechnol.* **2002**, *13*, 40–46.
(58) Ishii, Y.; Yanagida, T. *HFSP J.* **2007**, *1*, 15–29.

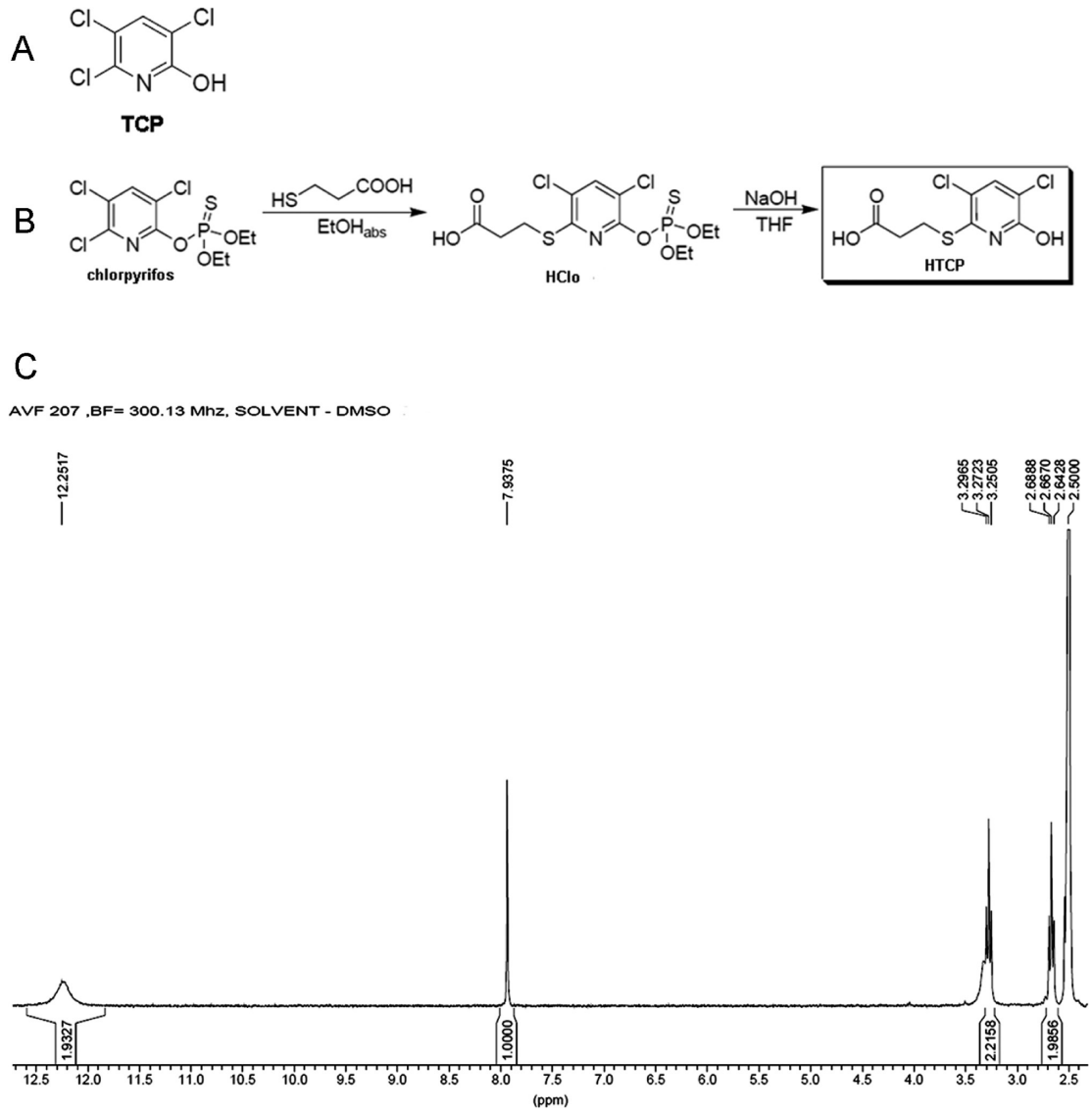

Figure 1. (A) Molecular structure of TCP. (B) Schematic illustration of strategy of derivation of TCP with a carboxyl group. (C) ^{1}H NMR (DMSO) spectrum of HTCP.

probes for fluorescent ITSA is highly innovative and important for environmental and clinical relevant applications. The advantages of such a quantum dot-based ITSA includes high sensitivity and stability because of the superior signal brightness and residence to photobleaching of quantum dots. Moreover, the quantum dot-based ITSA is, for the first time, integrated with a portable fluorescence reader, which might provide a simple, portable, rapid, and sensitive field biomonitoring tool.

In this article, we report on a portable quantum dot-based fluorescent ITSA for simple, sensitive, and selective biomoitoring of trichloropyridinol (TCP, Figure 1A) in rat plasma. We use TCP as a model analyte because it is a metabolite of chlorpyrifos (CPF), one of the most widely used organophosphorus pesticides in agriculture across the world.[59−61] TCP is used as a biomarker of CPF exposure. Therefore, it is important to develop a portable biosensor for simple, sensitive, selective, and quantitative analysis of TCP.[61,62] We have extensively studied biological matrixes such as rat plasma and saliva for CPF biomonitoring utility,[63,64] and rat plasma was utilized as a model biomonitoring matrix in this study. The approach developed in this work combines the advantage of the ITSA and the high sensitivity and the stability of quantum dot resulting in a novel, portable, and rapid competitive immunoassay tool for sensitive and selective detection of TCP. Thus, this sensor platform may open up a new avenue for rapid point-of-care (POC) screening, environmental biomonitoring, and clinical diagnosis.

EXPERIMENTAL SECTION

Reagents and Materials. Mouse monoclonal TCP antibody was obtained from Strategic Diagnostics Inc. (Newark, Delaware). TCP, phosphate buffer saline (PBS, 0.01 M), bovin serum albumin

(59) Choi, K.; Joo, H.; Rose, R. L.; Hodgson, E. *J. Biochem. Mol. Toxicol.* **2006**, *20*, 279–291.
(60) Kim, J. R.; Ahn, Y. J. *Biodegradation* **2009**, *20*, 487–497.
(61) Mauriz, E.; Calle, A.; Manclus, J. J.; Montoya, A.; Lechuga, L. M. *Anal. Bioanal. Chem.* **2007**, *387*, 2757–2765.
(62) Liu, G. D.; Riechers, S. L.; Timchalk, C.; Lin, Y. H. *Electrochem. Commun.* **2005**, *7*, 1463–1470.
(63) Timchalk, C.; Campbell, J. A.; Liu, G.; Lin, Y.; Kousba, A. A. *Toxicol. Appl. Pharmacol.* **2007**, *219*, 217–225.
(64) Smith, J. N.; Wang, J.; Lin, Y.; Timchalk, C. *Toxicol. Sci.* **2010**, *113*, 315–325.

(BSA), *N*-hydroxy-succinimide (NHS), Tween-20, and *N*,*N*′-dimethylformamide (DMF, 99.8%) were purchased from Sigma-Aldrich (St. Louis, MO). 1-Ethyl-3-(3- dimethylaminopropyl)carbodiimide (EDC) was purchased from Fluka (St. Louis, MO). Casein was purchased from Bio-Rad (Hercules, CA). Nitrocellulose membrane, absorbent pad, sample pad, and conjugation pads as well as backing cards were purchased from Millipore (Temecula, CA). NAP-5 columns were purchased from GE Healthcare UK Limited. QD 655 (CdS@ZnS) was purchased from Invitrogen (Eugene, OR). All chemicals used in this study were analytical reagent grade. All stock solutions were prepared using deionized water purified with the Nanopure System (Barnstead, Kirkland, WA).

Derivatization of TCP with Carboxyl Functional Group. The TCP derivatized with carboxyl functional group (HTCP) was synthesized according to previous literature with a slight modification.[65,66] Briefly, HTCP was prepared from chlorpyrifos by substitution of the chlorine in position 6 by a 3-mercaptopropionic acid spacer arm (product so-called HClo), followed by hydrolysis of the thiophosphate ester (Figure 1B). To a solution of 3-mercaptopropionic acid (36.3 g, 340 mmol) in $EtOH_{abs}$ (100 mL), solid KOH (38.1 g, 680 mmol) was added and heated until dissolved. Then, chlorpyrifos (250 mL of a 48% soln., 120.0 g, 340 mmol) dissolved in $EtOH_{abs}$ (100 mL) was added. After the reaction mixture was heated to reflux (1 h), the solvent was removed under reduced pressure to give 224.1 g of yellow oily residue (HClo) which was used for the next step without further purification.

To a stirred solution of HClo (224.12 g) in THF (300 mL), an aqueous solution of 1 M NaOH (2000 mL) was added and the mixture was refluxed (1 h). After the reaction mixture was extracted with methyl tertiary butyl ether (MTBE, 2 × 200 mL), the aqueous layer was acidified to pH 4 and the mixture was kept overnight. The precipitate was filtered out and dried in an oven (50 °C, 1.5 h) to give crude HTCP as a light-yellow solid. After recrystallization from *n*-BuOH three times, 5.9 g (6.5% yield over two steps) of pure HTCP as pale yellow leaves was obtained. ^1H NMR (DMSO) data in Figure 1C confirms that the carboxyl functional group has successfully linked to a TCP molecule: δ 7.94 (s, 1H, ArH), 3.27 (t, 2H, SCH_2), 2.66 (t, 2H, CH_2COO), 12.25 (s, 2H, OH).

Synthesis of TCP−Quantum Dot Conjugates. The TCP−QD conjugate was prepared by EDC-facilitated conjugation (Figure 4A). First, TCP was preactivated by adding 500 μL of 0.2 M NHS and 500 μL of 0.2 M EDC to 1 mL of 0.1 M TCP in dry DMF, and the resulting solution was incubated at room temperature under gentle shaking for 1 h. Then, to 50 μL of the above preactivated TCP solution was added 60 μL of 8 μM amino-modified QD and 390 μL of 0.1 M sodium bicarbonate buffer (pH 8.1), and the resulting solution was incubated under the same conditions for 2 h. The resulting solution was subjected to NAP-5 column separation to remove excess unconjugated TCP and other small molecules. Finally, the collected TCP−QD solution was concentrated by a 30K centrifugal tube (7000 rpm) for 15 min and reconstituted to a final volume of 500 μL with 0.01 M PBS buffer containing 3% BSA and 0.02% Tween-20 and stored at 4 °C. Here, BSA and Tween-20 were added into the solution of TCP−quantum dot conjugates to reduce the nonspecific adsorption of quantum dots in the membrane. The number of TCP per QD was calculated by comparing the concentration of TCP and the concentration of QD in the conjugate solution. The concentration of TCP in the TCP−QD conjugate solution was calculated by comparing the UV−vis absorption at 330 nm of TCP−QD conjugate solution to that of a series of standard TCP solution. The concentration of QD was calculated by comparing the fluorescence signal at 655 nm of the TCP−QD solution to that of a series of standard QD solution. On average, 30 TCP molecules were linked to a single QD.

Rat Plasma Collection. Adult male Sprague-Dawley rats (300−400 g) were purchased from Charles River Laboratories Inc. (Raleigh, NC). Rats were housed in solid bottom cages with hardwood chips under standard laboratory conditions. Water and feed (PMI 5002, Certified Rodent Diet) were provided ad libitum. Rats were humanely euthanized using CO_2, and blood was collected via cardiac puncture. Sodium heparin was used as an anticoagulant, and blood was centrifuged at 1600*g* for 10 min to separate plasma from the packed red blood cell fraction. All procedures involving animals were in accordance with protocols established in the National Research Council (NRC) Guide for the Care and Use of Laboratory Animals and were reviewed by the Institutional Animal Care and Use Committee of Battelle, Pacific Northwest Division.

Preparation of TCP-Spiked Rat Plasma Samples. TCP-spiked rat plasma samples were prepared by spiking a series of different concentrations of standard TCP in 10-fold diluted rat plasma with PBS. Rat plasma without addition of standard TCP served as a control.

Test Strip Preparation. A TCP competitive assay test strip consists of five components: sample application pad, conjugate pad, nitrocellulose membrane, absorbent pad, and backing card. The preparation of TCP test strip was described as follows. The sample application pad (20 mm × 30 cm) and the conjugation pad (8 mm × 30 cm) were both made of glass fiber. The conjugation pad was first treated by dispensing a desired volume of buffer (pH 7.4) containing 0.01 M PBS, 3% BSA, 10% sucrose, and 0.25% Tween-20 with the dispenser XYZ-3050 AirJet Quanti 3000. The pad was dried at room temperature for 2 h. Then, a desired volume of diluted TCP−QD conjugate solution was dispensed on the conjugation pad with the dispenser XYZ-3050 BioJet Quanti 3000, dried at 4 °C for 1 h, and stored in the same condition. The test zone of the strip was prepared by dispensing a desired volume of 1 mg/mL mouse monoclonal TCP antibody solution with the dispenser XYZ-3050 BioJet Quanti 3000 onto a nitrocellulose membrane (40 mm × 30 cm). After 1 h of drying at 4 °C, the membrane was blocked with 1% casein at 4 °C for 1 h, dried at room temperature under vacuum for 30 min, and then stored at 4 °C. Such a blocking treatment here is to reduce the nonspecific binding of quantum dots and increase the mobility of the quantum dots on the membrane. Both the sample pad and the absorbent pad (20 mm × 30 cm) were stored at room temperature without any treatments. All of the above four parts were assembled on a plastic adhesive backing card (60 mm × 30 cm) using the Batch Laminating System LM5000. Each part overlapped 2 mm to ensure the solution migrating through the strip during the assay. Finally,

(65) Manclus, J. J.; Montoya, A. *J. Agric. Food Chem.* **1996**, *44*, 3710–3716.
(66) Manclus, J. J.; Primo, J.; Montoya, A. *J. Agric. Food Chem.* **1994**, *42*, 1257–1260.

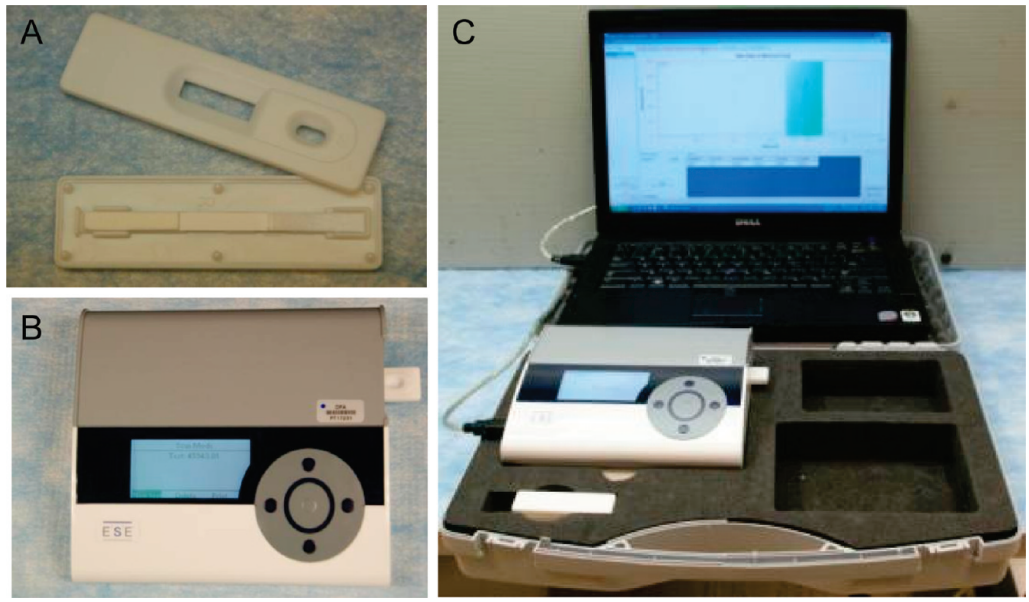

Figure 2. Photograph of (A) the test strip in the cassette, (B) portable test strip reader integrated with test strip in the cassette shown in (A), and (C) the entire immunosensor system including a connected laptop.

the TCP test strips with a 4 mm width were cut using the Guillotine Cutting System CM 4000 and assembled in the strip cassettes (Figure 2A) for the testing and reading.

Instrumentation. The test strip fabrication system consists of a XYZ-3050 Dispenser, LM5000 Laminator, and the Guillotine Cutting System CM 4000 which were purchased from BioDot LTD (Irvine, CA). The XYZ-3050 Dispenser includes an AirJet Quanti 3000 dispenser and a BioJet Quanti 3000 dispenser. A portable test strip reader ESE-Quant FLUO (Figure 2B), which can be connected to a laptop, was purchased from DCN Inc. (Irvine, CA) to collect the fluorescence signal of the assay on the test strip. The entire sensor system can be housed in a small case (Figure 2C). The characterization of TCP−QD conjugate was carried out by measurements of absorption spectra and fluorescence spectra on a microplate reader Safire 2 (TECAN, Durham, NC). A benchtop centrifuge Eppendorf 5804 (Eppendorf, Germany) and Amincon Ultra 30K centrifuge tubes (Millipore, Billerica, MA) were purchased for concentration and separation of TCP−QD conjugate. Proton nuclear magnetic resonance (^{1}H NMR) spectra were obtained with a Varian VR-400S spectrometer (Sunnyvale, CA) that was operated at 400 MHz. X-ray photoelectron spectroscopy (XPS) measurements were performed with a Physical Electronics Quantum 2000 Scanning Microprobe. This system uses a focused monochromatic aluminum Kα X-ray (1486.7 eV) source for excitation and a spherical section analyzer. A 100 W X-ray beam focused to a diameter of 100 μm was rastered over a 1.3 mm × 0.2 mm rectangle on the sample. High-energy resolution data were collected using pass energy of 46.95 eV. For the Ag 3d5/2 line, these conditions produced a full-width half-maximum of 0.98 eV. The binding-energy scale was calibrated using Cu 2p3/2 at 932.62 ± 0.05 eV and Au 4f at 83.96 ± 0.05 eV.

Fluorescent Immunochromatographic Assay of TCP. The competitive assay on the test strip was performed as follows: 50 μL of sample solution in PBS buffer containing desired concentrations of TCP were added to the sample application pad. PBS buffer or plasma without TCP was used as a control. After an adequate incubation (e.g., 15 min), the competitive immunoreactions between TCP and TCP−QD binding to TCP antibody on the test zone were completed. Then, the strip cassette was inserted into the reader ESE-Quant FLUO, and the fluorescence signal from the quantum dots on the test zone was recorded accordingly.

RESULTS AND DISCUSSION

Principle of the Method. In this study, the principle of the competitive ITSA is based on competitive binding between the various amount of analyte (sample, TCP in this paper) and a fixed amount of competitor (labeled TCP analog, TCP−QD in this paper) to the limited amount of capturing antibody (TCP antibody in this paper) on the test zone. Basically, there are four steps during this competitive immunoassay (Figure 3). A certain amount of analyte solution is first applied to the sample application pad (Figure 3A). Then capillary action causes liquid sample to migrate toward the other end of the strip. As the liquid sample migrates into the conjugation pad, the analyte and the competitor mix together and continue to migrate along the strip by capillary action (Figure 3B). When these mixtures reach the test zone, analytes and competitors competitively bind to the capturing antibodies which are immobilized on the test zone. The fluid fraction containing excess analytes and competitors continue to flow into the absorbent medium at the end of the strip. In a control assay (no analyte), competitors are fully binding to the antibodies in the test zone (Figure 3C). After a complete assay, the test strip is subjected to fluorescence detection with the test strip reader (Figure 3D). The more analytes in the sample, the less QD-labeled competitors would bind to the capturing antibodies in the test zone, which leads to fluorescence signal decrease. Therefore, the fluorescence signal will be inversely proportional to analyte concentrations in the sample, which can be used for quantitation of TCP in samples.

Characterization of Quantum Dot−TCP Conjugates. In this study, TCP was first derivatized with a carboxyl group to prepare

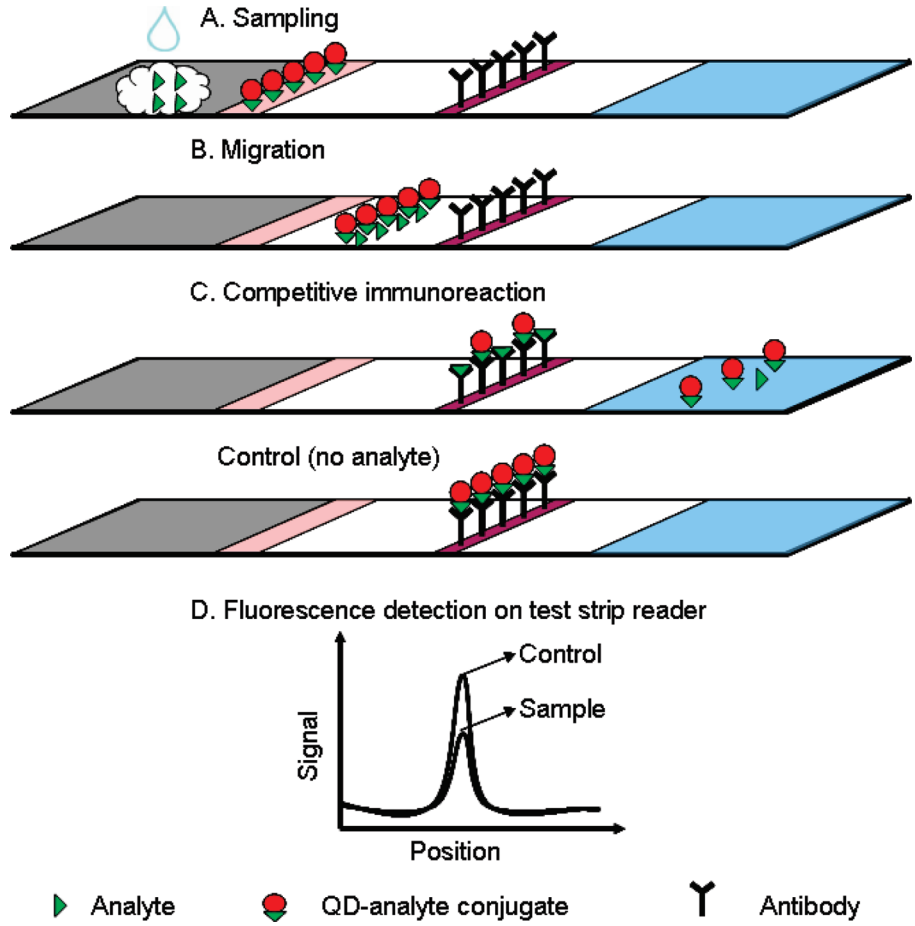

Figure 3. Schematic illustration of the principle of fluorescent ITSA. (A) Aqueous sample containing analytes was applied to the sample zone. (B) Analytes migrate together with QD-conjugated competitors toward the other end of test strip by capillary force. (C) Competitive immunoreactions among analytes, conjugated competitors, and antibodies. Excess conjugated competitors and analytes continue to migrate toward the absorption pad. In a control assay (no analyte), the QD-conjugated competitors are fully binding to the antibodies in the test zone. (D) Fluorescence detection on the test strip reader.

TCP−QD conjugates for the development of a competitive immunochromatographic fluorescence sensor. The derivatized carboxylic group of TCP facilitates the conjugation of TCP to the amino-functionalized QD surface. The conjugation was preceded using a standard procedure with the coupling reagent EDC (Figure 4A). The TCP−QD conjugates were characterized with XPS. Figure 4B displays XPS spectra of TCP, TCP−QD conjugate, and QD, respectively. It is obvious that both TCP (curve a) and TCP−QD conjugate (curve b) show the binding energy of the core electrons for the $C1_{2p}$ at 199−201 eV, which is attributed to the organic chloride groups (e.g., C_6H_5Cl).[67] On the other hand, no obvious signal can be detected on QD at such area of binding energy. These results indicate that TCP has been successfully conjugated to the QD surface.

The fluorescence characteristics of the TCP−QD conjugate were also studied. Figure 4C shows the typical fluorescence spectra of the QD (curve a) and the TCP−QD conjugate (curve b). One can see that a well-defined peak was observed from the TCP−QD conjugate, which is very similar to that of the QD except a slight shift (2 nm) of peak position, indicating that TCP does not affect the fluorescence characteristic of the QD. It is obvious that the fluorescence intensity of TCP−quantum dot conjugates is still strong enough. Therefore, the TCP−QD conjugate can be used on the test strip for this competitive immunoassay.

The binding affinity of the TCP antibody to the TCP−QD conjugate was further studied on the test strip. Two control experiments with BSA (instead of TCP antibody) in the test zone and the QD (without TCP) were performed under the same conditions. Figure 5 shows the fluorescence signals of the sensor obtained under different conditions: TCP−QD + TCP antibody, TCP−QD + BSA, and QD + TCP antibody. It is obvious that the maximum signal was obtained by incubating TCP−QD with TCP antibody. Much smaller signals in control experiments may come from the nonspecific adsorption of QD or TCP−QD conjugates. These results demonstrate that the TCP−QD conjugate can be specifically recognized by TCP antibody, indicating that QDs do not generate steric hindrance to the binding events, which is contributed to a thin layer of functionalized polymer on the surface of the QD, providing spacing between the TCP and the QD, therefore, greatly increasing the flexibility of TCPs on the surface of the QDs.

Optimization of Experimental Parameters. Certain parameters of the competitive immunoassay would affect the response of the immunosensor. The amount of TCP−QD conjugate in the conjugate pad directly influences fluorescent response of the immunosensor because the fluorescence signal depends on the

(67) Domazetis, G.; Raoarun, M.; James, B. D.; Liesegang, J.; Pigram, P. J.; Brack, N.; Glaisher, R. *Energy Fuels* **2006**, *20*, 1556–1564.

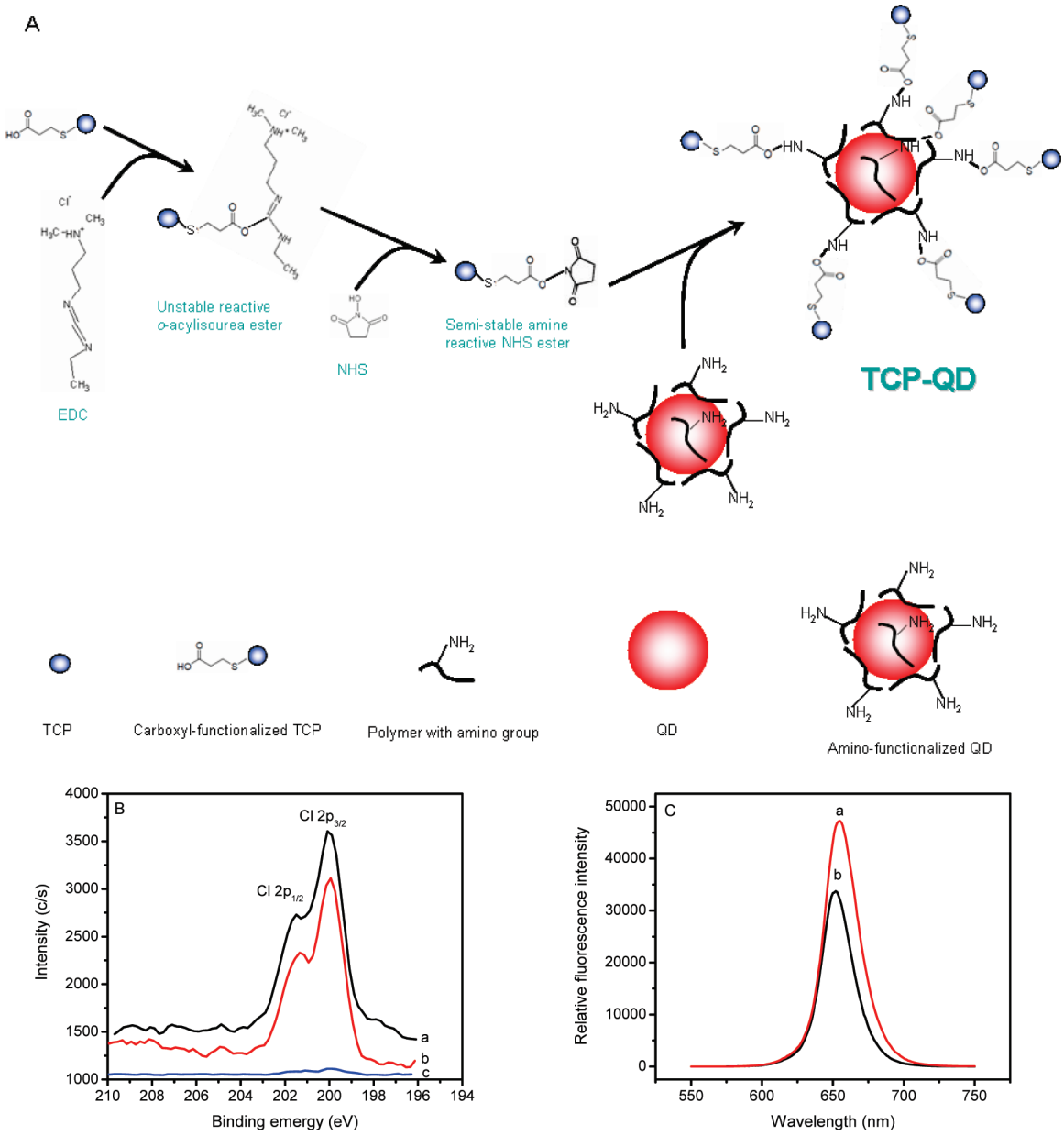

Figure 4. (A) Schematic illustration of conjugation of TCP to the QD surface. (B) XPS measurements of Cl_{2p} from TCP (a), TCP−QD conjugate (b), and QD (c). (C) Typical fluorescence spectra of 8 nM QD (a) and 100-fold diluted TCP−QD (b) in 0.01 M PBS.

amount of TCP−QD conjugate bound to TCP antibody immobilized on the test zone. Therefore, different dilution times of stock TCP−QD conjugate in the conjugate pad were studied. To determine the optimal amount of TCP−QD in the conjugated pad for the assay, fluorescence signals with different dilutions of stock TCP−QD were obtained using 10 ng/mL TCP and PBS (a control) in parallel (Figure 6A). The ratio of the signal from the TCP to BSA is shown in the inset of Figure 6A. As shown in Figure 6A, the fluorescent responses to both the samples (TCP) and the control decrease with greater dilution of the TCP−QD conjugate. As is shown in the inset of Figure 6A, however, the signal-to-control ratios reach to the minimum at a 600-fold dilution of the TCP−QD conjugate, indicating that the competition ability of TCP against TCP−QD is the strongest at this dilution ratio. Therefore, a 600-fold dilution of stock TCP−QD conjugate was routinely used in the conjugate pad throughout this study.

Another parameter affecting the fluorescent response of the immunosensor is the immunoreaction time. Figure 6B displays the fluorescent responses of the immunosensor to 100 ng/mL TCP under different immunoreaction times, where the responses to PBS were determined in parallel as the control. It can be seen from this figure that the fluorescent response increases sharply with the increase of immunoreaction time within the first 15 min and then tends to level off after 15 min, especially for the sample. Considering the time consumed and signal intensity, 15 min was routinely used for the following experiments.

It is important to evaluate the activity of the antibodies in the test zone to guard against the potential of false positive signals. In order to achieve this evaluation, a control sample (containing no TCP) is used to evaluate the activity of the antibodies in the test zone. If the antibodies have the activity, then the fluorescence should appear in the test line. This test can confirm that the

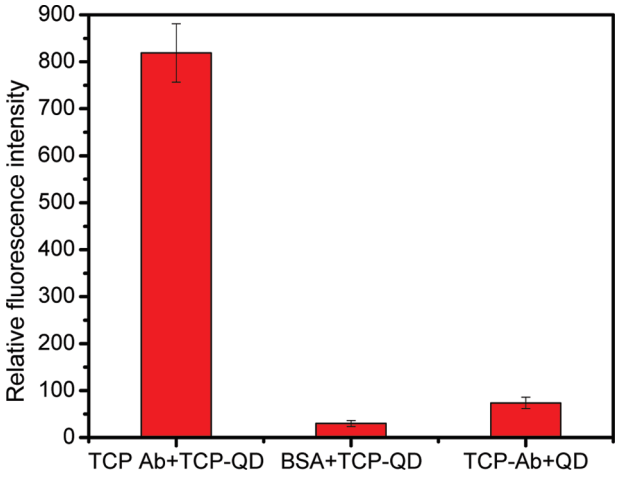

Figure 5. Fluorescent responses of the sensor applied with PBS buffer under the following conditions: TCP−QD immobilized in the conjugation pad and TCP antibody in the test zone (TCP Ab + TCP QD), TCP−QD in the conjugation pad and BSA in the test zone (BSA + TCP−QD), and QD in the conjugation pad and TCP antibody in the test zone (TCP Ab + QD). Immunoreactions were performed by applying 50 μL of 0.01 M PBS buffer to the sample application pad. Fluorescence signals were recorded after 15 min of immunoreaction.

antibodies in the test line have activity and work well. Otherwise, the test strip is out of function and should be discarded. We have investigated the biologic activity of antibodies on test strips by periodical testing of ITSAs using control samples and found that the activity of antibodies in the test zone can be maintained up to 6 months if stored properly (4 °C, sealed).

Analytical Performance of the Sensor. Under the optimal conditions, the performance of a QD-based fluorescence immunosensor for detecting TCP was further evaluated. Figure 7A shows the typical fluorescence signals of the sensor with increasing TCP concentrations (from top to bottom: 0, 1, 5, 10, 50, 100, 500, and 1000 ng/mL). It can be seen that the peak intensity decreases with the increase of TCP concentrations. Normalized signals expressed as 100 (F/F_0) (where F and F_0 are the peak fluorescence intensity obtained with the TCP analyte and the blank sample, respectively) were plotted versus the logarithm of TCP concentration. Figure 7B shows a sigmoidal shape of the calibration curve of TCP at the concentration range from 1 to 1000 ng/mL, with a linear range from 1 to 50 ng/mL ($Y = 90.68 - 50.76 \lg(X)$, $R = 0.9935$). A detection limit was estimated about 1.0 ng/mL from the linear equation based on a 90% F/F_0 normalized signal of the analyte concentration, which was comparable to the value indicated by the manufacturer of the TCP RaPID Assay Kit.[68] The reproducibility of such a fluorescent immunosensor was also studied by six duplicated measurements of TCP at different concentrations. Under current conditions, the relative standard deviations for 0 and 10 ng/mL TCP are 6.3% and 12.9%, respectively. The total analysis time is about 15 min. This quantum dot-based sensor offers great promise for a simple, rapid, and sensitive field biomonitoring of TCP in biological samples.

In Vitro Evaluation in Rat Plasma. To explore its clinical application, this fluorescent immunosensor was evaluated with a

(68) Strategic Diagnostics Inc. Trichloropyridinol RaPID Assay; http://www.sdix.com/PDF/Products/ratcp.pdf.

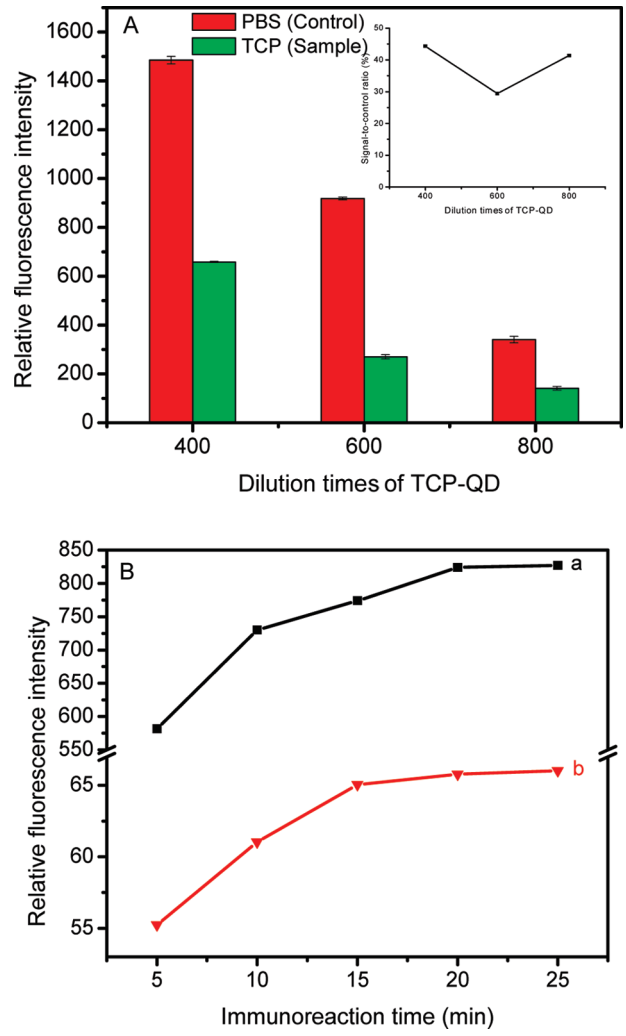

Figure 6. Optimization of parameters of the immunosensor. (A) Effect of dilution times of the stock TCP−QD conjugate on the fluorescent responses of ITSA. TCP−QD conjugates with different dilutions were dispensed onto the conjugation pad. The ITSA was performed by applying 50 μL of PBS (control) or 10 ng/mL TCP to the sample application pad. Fluorescence signals were recorded after 15 min of immunoreaction. The inset shows the signal-to-control ratios under different dilution times of the TCP−QD conjugate. (B) Effect of immunoreaction time on the fluorescent responses of ITSA. The ITSA was performed by applying 50 μL of (a) PBS (control) or (b) 100 ng/mL TCP to the sample application pad. Fluorescence signals were recorded at different immunoreaction times.

rat plasma sample spiked with standard TCP. To reduce the matrix effect, we diluted the plasma by 10-fold. These experiments were carried out by spiking a series of different concentrations of standard TCP in diluted rat plasma (10 times with PBS). Rat plasma without addition of standard TCP served as a control. These samples were applied to this fluorescent immunosensor, and the fluorescence signals were recorded by the test strip reader. A similar calibration curve was obtained, as showed in Figure 8. TCP concentrations spiked in rat plasma samples were calculated based on the fluorescence signals and the calibration curve. Table 1 displays recovery of different concentrations of TCP spiked in plasma obtained by the quantum dot-based fluorescent ITSA. The average recovery for these spiked samples between 1 and 50 ng/mL was 102.0%, indicating that this sensor can be used for biomonitoring of TCP in biological samples. Results demon-

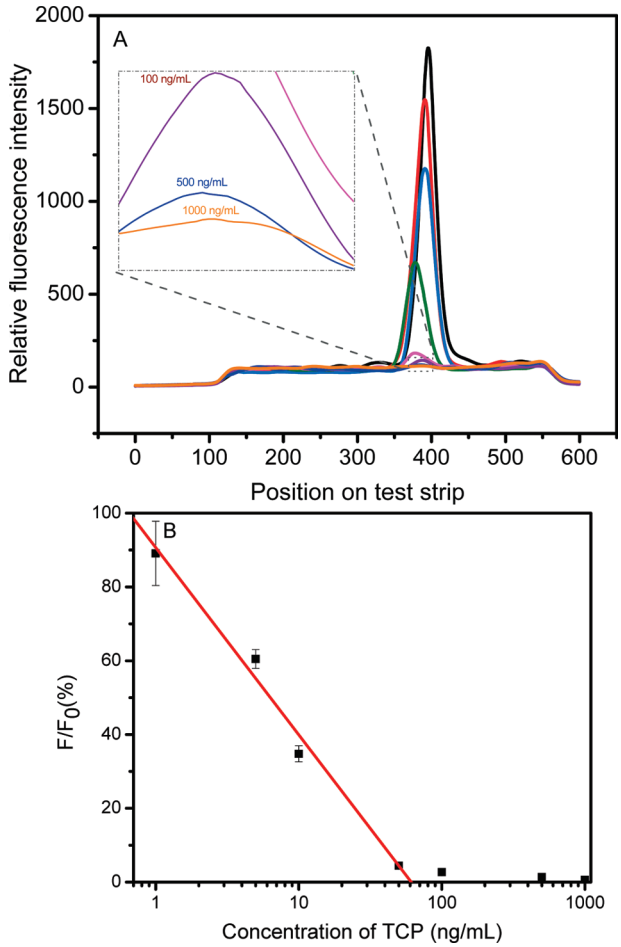

Figure 7. (A) Typical fluorescent responses of the immunosensor with increasing TCP concentrations, from top to bottom: 0, 1, 5, 10, 50, 100, 500, and 1000 ng/mL, respectively. Immunoreaction time was 15 min. The inset is the enlargement of the fluorescent responses to 100, 500, and 1000 ng/mL TCP, respectively. Other conditions were the same as in Figure 6B. (B) The resulting calibration curve of TCP. Normalized signals expressed as 100 (F/F_0) (where F and F_0 are the peak fluorescence intensity obtained with the TCP analyte and the blank sample, respectively) were plotted versus the logarithm of TCP concentration.

strate that this fluorescent immunosensor has a potential for sensitive, rapid, and POC biomonitoring for chlorpyrifos exposure.

CONCLUSIONS

We have successfully developed a portable quantum dot-based fluorescent immunosensor for simple, rapid, and sensitive biomonitoring of TCP, a primary metabolite biomarker of the pesticide chlorpyrifos. The fluorescent ITSA used in this sensor takes advantage of the speed and low cost of the conventional immunochromatographic strip test and high sensitivity of the nanoparticle-based fluorescent immunoassay. Under optimal conditions, this sensor is capable of detecting a minimum 1.0 ng/mL TCP standard analyte in 15 min and is capable of detecting TCP spiked in rat plasma with an average recovery of 102.0%. Results demonstrate that this sensor provides a rapid, clinically accurate, and quantitative tool for TCP detection. In the future, the immunosensor will be more fully validated in vivo to quantify chlorpyrifos exposure. In addition, the immunosensor will be adapted to detect protein biomarkers as indicators of exposure

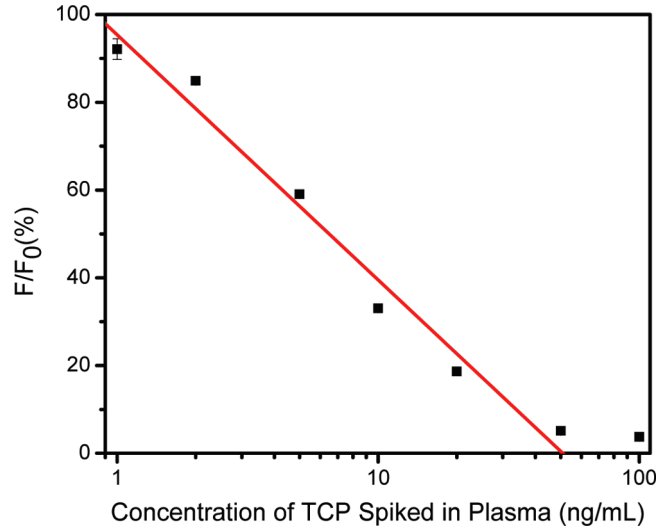

Figure 8. Normalized signals with increasing TCP spiked in plasma. The plasma was 10-fold diluted, and then different amounts of TCP standard were spiked into this diluted plasma to final concentrations of 1, 2, 5, 10, 20, 50, and 100 ng/mL. The immunoassay conditions were the same as in Figure 7A.

Table 1. Recovery of TCP Spiked in Plasma Samples Obtained by the Quantum Dot-Based Fluorescent ITSA

TCP spiked in plasma (ng/mL)	TCP found by ITSA (ng/mL)	recovery (%)
1	1.14	114.0
2	1.54	77.0
5	4.47	89.4
10	13.04	130.4
20	23.61	118.1
50	41.31	82.6

and biological response. Therefore, this sensor may open up opportunities for versatile in-field and POC testing and screening of metabolite/protein biomarkers.

ACKNOWLEDGMENT

This work was conducted at Pacific Northwest National Laboratory (PNNL) and supported partially by Grant R01 OH008173-01 from the Centers for Disease Control/National Institute for Occupational Safety and Health, NIH, and Grant Number U01 NS058161-01 from the National Institutes of Health CounterACT Program through the National Institute of Neurological Disorders and Stroke, NIH. The contents of this publication are solely the responsibility of the authors and do not necessarily represent the official views of the federal government. The characterization work was performed at the Environmental Molecular Sciences Laboratory (EMSL), a national scientific user facility sponsored by the Department of Energy's Office of Biological and Environmental Research located at Pacific Northwest National Laboratory. PNNL is operated for DOE by Battelle under Contract DE-AC05-76L01830. Z.Z. would like to acknowledge the fellowship from the China Scholarship Council and the fellowship from PNNL.

Received for review January 29, 2010. Accepted May 10, 2010.

AC100260M